Vietnam Journal of Earth Sciences, 43(1), 13-22, https://doi.org/10.15625/0866-7187/15572

Vietnam Academy of Science and Technology
Vietnam Journal of Earth Sciences
http://www.vjs.ac.vn/index.php/jse

Finite element modeling of fluid flow in fractured porous media using unified approach

Hai-Bang Ly*, Hoang-Long Nguyen, Minh-Ngoc Do

University of Transport Technology, Hanoi 100000, Vietnam

Received 9 March 2020; Received in revised form 21 April 2020; Accepted 15 October 2020

ABSTRACT

Understanding fluid flow in fractured porous media is of great importance in the fields of civil engineering in general or in soil science particular. This study is devoted to the development and validation of a numerical tool based on the use of the finite element method. To this aim, the problem of fluid flow in fractured porous media is considered as a problem of coupling free fluid and fluid flow in porous media or coupling of the Stokes and Darcy equations. The strong formulation of the problem is constructed, highlighting the condition at the free surface between the Stokes and Darcy regions, following by the variational formulation and numerical integration using the finite element method. Besides, the analytical solutions of the problem are constructed and compared with the numerical solutions given by the finite element approach. Both local properties and macroscopic responses of the two solutions are in excellent agreement, on condition that the porous media are sufficiently discretized by a certain level of finesse. The developed finite element tool of this study could pave the way to investigate many interesting flow problems in the field of soil science.

Keywords: Finite element method, fractures porous media, transport properties, permeability.

1. Introduction

In many problems related to soil science, characterizing fluid flow in fractured porous media is one of many challenges that researchers have to face (Auriault and Boutin, 1994, 1993, 1992; de Borst, 2017). Theoretical and applied researches have received increased attention due to the importance of the research area (de Borst, 2017). Indeed, the existence and propagation of fractures in porous media can be both desirable or undesirable, depending on specific applications. The presence of fractures is unlikely, for instance, in the storage of wastes in soils, rocks (Bachu, 2008), or filtration applications (Herzig et al., 1970). However, fractures can be a critical element for hydraulic fracturing in the oil and gas industry as they can act as channels for the fluids can flow more easily (Rahm, 2011). Many applications, taking advantage of such behavior, have been applied for the use in materials science (Bose et al., 2012; H. B. Ly et al., 2015; Ly et al., 2016a). Moreover, studying the transport phenomena through

*Corresponding author, Email: banglh@utt.edu.vn

fractured porous media raises several fundamental and practical questions, such as the role of the fractures and porous media, its relationship to the transfer process, to the final flow behavior of the porous media. Thus, the transport mechanism through the fractures and the surrounding porous media requires an in-depth investigation (Dietrich et al., 2005).

In the literature, the determination of the permeability of porous media has been addressed by several approaches, for instance, asymptotic expansions (Auriault and Sanchez-Palencia, 1977), volume average methods (Whitaker, 1967), analytical approach (Monchiet et al., 2019; Wang, 2003, 2001), Fast Fourier transform - FFT (Ly et al., 2016b; Monchiet et al., 2009; Nguyen et al., 2013), Lattice-Boltzmann method (Pan et al., 2004), or using the finite element approach - FEM (Burman and Hansbo, 2007; Correa and Loula, 2009; H.-B. Ly et al., 2015). Based on FFT or FEM, the two numerical schemes solve the elementary cell problem to determine the macroscopic permeability of fractured porous media. Treating flow problems using FEM, two approaches have been developed, including a "unified" and a "decoupled" one. The decoupled approach uses different discretization spaces dedicated to the fractures and the porous medium, for instance, in (Discacciati et al., 2007), (Layton et al., 2002) or (Celle et al., 2008). In a unified approach, the finite element discretization is based on the same finite element spaces (and similar elements) for the fractures and the porous medium. This method is based on the use of a “robust” element, or modified variational formulation of the flow problem (Arbogast and Brunson, 2007; Correa and Loula, 2009; Karper et al., 2009; Xie et al., 2008) while the decoupled strategy is based on the use of two matching meshes and two finite element spaces for discretizing the flow problem.

In this study, the unified approach in solving flow problems using FEM is considered. Based on the theoretical development of the work of (Arbogast and Brunson, 2007), a FEM-based numerical tool is developed and validated. This paper is presented as follow: (i) a brief introduction of the flow in fractured porous media is presented in Section 1; (ii) the nature of the flow in fractured porous media is presented in Section 2; (iii) a FEM variational formulation and numerical integration scheme is presented in Section 3; (iv) analytical solutions for a specific problem is given in Section 4; and (v) results and comparisons with the developed FEM-based numerical tool is introduced in Section 5 and 6, following by a conclusion and several perspectives.

2. Couling free fluid with flow in porous media

The nature of coupling free fluid with flow in porous media leads to a well-known problem of coupling the Stokes and Darcy equations. In this study, the numerical scheme of the coupling process is performed using the finite element method in a unit cell problem. It can be seen that in such a unit cell, three separated scales exist: (i) the scale of the smallest pores in the porous media, or the lower scale, (ii) the scale of the fractures or the intermediate scale, (iii) and the macroscopic scale where the pressure is applied to generate the flow. The permeability of the lower scale is denoted as K_D, represents the permeability that is homogenized by the Darcy equations. In the fractures, the flow is described by the Stokes equations. At the interface between the Stoke region and the Darcy region, the adherence condition is applied, representing the continuous/discontinuous fields (i.e., the velocity field and the pressure field) across

such an interface. Considering the macroscopic scale, the macroscopic permeability is computed in coupling the free fluid in the fractures (Stokes equations) and flow in porous media (Darcy law). Finally, the velocity field and pressure field are obtained at this step, along with the effective transport property of the porous media. Fig. 1 represent a schema of the fractured porous media containing the porous phase, the fluid phase, and the interface between the two regions.

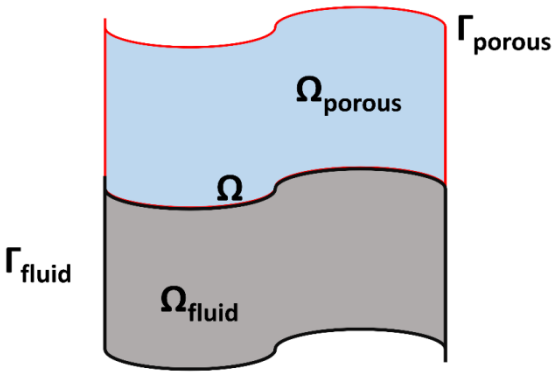

Figure 1. Representation of the fractured porous media

The porous medium considered in this study is supposed saturated by a homogeneous viscous fluid, Newtonian, and dynamic viscosity μ_f. The unit cell problem is a rectangle in two dimensions using spatial invariance of two vectors. The total volume of the unit cell is $\Omega_{total} = \Omega_{porous} \cup \Omega_{fluid}$, whereas the interface (or the surface) between fractures and the porous medium is denoted as Ω. For the sake of simplicity, the notation Ω_{fluid} is denoted as Ω_f, and Ω_{porous} is denoted as Ω_p. In the porous phase, the fluid obeys the Darcy equations as follow:

$$\begin{cases} \frac{\mu_f}{K_D} v_p(\underline{x}) - \nabla p_p(\underline{x}) - \underline{G} = 0 \quad \forall \underline{x} \in \Omega_p \\ \nabla v_p(\underline{x}) = 0 \quad \forall \underline{x} \in \Omega_p \end{cases} \quad (1)$$

where $\underline{G}$ is the applied pressure gradient, $v_p(\underline{x})$ and $p_p(\underline{x})$ are the velocity and pressure fields in the porous region. In the fractures, the fluids flow freely and obey the Stokes equations:

$$\begin{cases} \mu_f \Delta v_f(\underline{x}) - \nabla p_f(\underline{x}) - \underline{G} = 0 \quad \forall \underline{x} \in \Omega_f \\ \nabla v_f(\underline{x}) = 0 \quad \forall \underline{x} \in \Omega_f \end{cases} \quad (2)$$

where $v_f(\underline{x})$ and $p_f(\underline{x})$ are the velocity and pressure fields in the fractures. At the interface Ω between the fractures and porous medium, the Beavers-Joseph-Saffman is applied (Beavers and Joseph, 1967; Mikelic and Jäger, 2000), and such a condition is given by:

$$\begin{cases} v_f(\underline{x})\underline{n} = v_p(\underline{x})\underline{n} \quad \forall x \in \Omega \\ 2\underline{n}Dv_f(\underline{x})\underline{t} = -\frac{\alpha}{K_D} v_f(\underline{x})\underline{t} \quad \forall x \in \Omega \\ 2\mu_f \underline{n}Dv_f(\underline{x})\underline{n} = p_f(\underline{x}) - p_p(\underline{x}) \end{cases} \quad (3)$$

where $\underline{n}$ and $\underline{t}$ are the normal and tangential vectors on the surface Ω, and D represents the symmetric gradient. Eq. (1) shows the continuity of the flux across the interface Ω, whereas Eqs. (2), (3) show a discontinuity related to both the velocity and pressure fields by the jump of the corresponding tangential components. In the formulation presented by Beavers-Joseph-Saffman, a coefficient α is introduced, representing the discontinuity of the fields. According to the authors, such a coefficient is difficult to determine using the classical approach (i.e., homogenization approach or experimental approach). In this study, infinite value of α is given to eliminate the tangential components of the velocity field across the interface. Finally, in taking the average value in the unit cell problem, the average value of the velocity field is obtained as the following equation:

$$\mathbf{V} = \langle v(\underline{x}) \rangle_{\Omega \cup \Omega_f \cup \Omega_p} = -\frac{1}{\mu_f} K \underline{G} \quad (4)$$

where $\mathbf{V}$ is the velocity field at the macroscopic scale, and K is the permeability at the macroscopic scale.

3. Variational formulation and numerical integration

In the finite element method, a variational formulation needs to be developed. Considering the unit cell problem, the coupling of free fluid and fluids flow in porous media can be formulated using a unique variational principle. The weak formulation of the coupling problem is written, for the solution (v,p) in introducing the test functions (w, q) such that:

$$\begin{cases} 2\mu_f \left(Dv_f, Dw_f\right)_f + \mu_f \left\langle \frac{\alpha}{\sqrt{K_D}} v_f \underline{t}, w_f \underline{t} \right\rangle_\Omega + \mu_f \left(\frac{1}{K_D} v_p, w_p \right)_p - \left(p, \nabla w\right) = \left(\underline{G}, w\right) \\ \left(\nabla v_p, q\right) = \left(0, q\right) \end{cases} \quad (5)$$

In Eq. (5), it is worth noticing that the two forms (*,*) and <*,*> denote the inner product or the duality pairing. A classical discretization of Eq. (5), using the finite element method, gives a linear system to solve:

$$[\mathbf{K}]\,[\mathbf{V}] = [\mathbf{F}] \quad (6)$$

where [**K**] is the assembly matrix containing the velocity field and pressure field in both the fractures and porous medium, [**V**] is the unknown nodal velocity and pressure of the mesh, and [**F**] demonstrates the pressure gradient that applied to the unit cell at the macroscopic scale. In order to construct [**K**], it is crucial to identify the phase of the element in the finite element mesh. If the element belongs to the fluid (or fractures) region, the first term of Eq. (5) should be used. If the element belongs to the porous medium, the third term of Eq. (5) should be utilized, and the second term should be applied to the nodal values that belong to the interface Ω.

The unit cell, dimensions (–L/2, L/2) × (–L/2, L/2), is discretized by square elements in a regular grid (N × N pixels). The periodicity condition is applied to the unit cell for the local velocity and pressure field. Such periodicity condition is written for the local velocity field as:

$$\begin{cases} v\,(-L, y) = v\,(L, y) \\ v\,(x, -L) = v\,(x, L) \end{cases} \quad (7)$$

and for the local pressure field as:

$$\begin{cases} p\,(-L, y) = p\,(L, y) \\ p\,(x, -L) = p\,(x, L) \end{cases} \quad (8)$$

The Lagrange multiplier (denoted as λ) is then applied to take into account the periodicity conditions. Then, the final system (Eq. (6)) is resolved by a direct method to get a better and high-quality solution. Fig. 2 present the discretization element of the local velocity field. Each corner of the element is described by two degrees of freedom (DOF), representing the flow of fluids in the two directions. Each edge of the element is described by a degree of freedom, representing the flux across the element. Overall, 12 DOFs are presented in the discretization element. It is worth noticing that this type of element is reported to satisfy the inf-sup condition (Arbogast and Brunson, 2007). Besides, the pressure field is discretized by a piecewise constant function in each square element, making one additional DOF related to the pressure field in each discretization element.

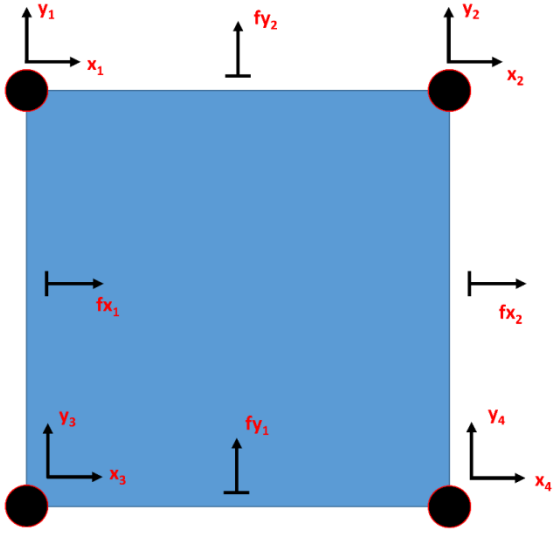

Figure 2. Degrees of freedoms of the rectangular element

4. Development of analytical solution

The development of an analytical solution for the problem of fluid flow in porous media is reported in this section. Similar to the previous sections, the fluid considered in this study is an incompressible Newtonian fluid. In the unit cell, the boundary conditions are considered symmetry, and the no-slip condition is considered at the fluid-porous interface. The unit cell problem of the analytical solution is presented in Fig. 3. The laminar flow leads to a problem of transversely isotropic, where two components of K can be found: K_1 and K_2 for each flow following the direction O_1 (the longitudinal flow) and O_2 (the transversal flow), respectively. The permeability K_1 can be obtained by applying a pressure gradient along the longitudinal direction (O_1), whereas K_2 can be computed with a pressure gradient along the transversal direction (O_2). Two other components of the permeability tensor, the off-diagonal components of K, are null.

For the unit cell problem, the permeability following the direction O_1 is:

$$K_1 = K_f + K_p \quad (9)$$

where K_f and K_p represent the permeability contributed by the fluid and the porous medium, obtained by averaging the velocity field on the volume of each region, respectively. The analytical formulations of K_f and K_p are:

$$K_f = L_f/L_c$$
$$K_p = (L_c\text{-}L_f)K_D/L_c \quad (10)$$

In Eq. (10), L_c and L_f are defined in Fig. 3, representing the dimensions of each region. In the fluid region, the flow is the laminar flow and has a parabolic velocity profile as a classical Poiseuille flow. The profile and the maximum velocity in the fluid phase are:

$$v(y) = \frac{\Delta p}{2\mu}\left(\frac{L_f^2}{4} - y\right)$$
$$v_{max} = \frac{\Delta p}{2\mu}\frac{L_f^2}{4} \quad (11)$$

Similarly, the permeability following the direction O_2 is:

$$K_2 = (L_c\text{-}L_f)K_D/L_c \quad (12)$$

It is noticed that such a developed analytical solution is the two-dimensional unidirectional flow of infinite extent, also called the plane Poiseuille flow.

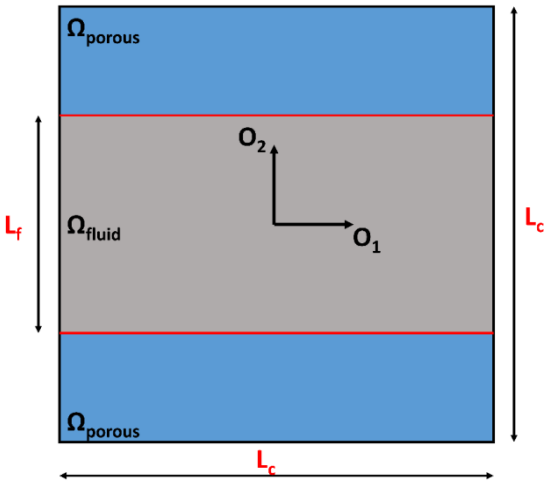

Figure 3. Schema of the plane Poiseuille flow

5. Results

The verification of the developed finite element tool is performed in this section. The fluid flow through fractured porous media is induced by a dimensionless pressure gradient (of 1 unit), the dynamic viscosity of the fluid is considered as dimensionless (of 1 unit), and the unit cell size is taken as 1 (from -0.5 to 0.5). First, the discretization choice is analyzed and compared with the analytical solutions. The results are presented in Table 1. In the case of transversal flow through the unit cell, it can be seen that the discretization choice of 200 × 200 pixels is sufficient to describe the flow in the fractures, whereas the flow in the porous media can be estimated precisely with only 50 × 50 pixels. Besides, in the case of longitudinal flow, a minimum discretization of 200 × 200 pixels is needed to describe the flow in fractures, and a discretization choice of 200 × 200 pixels is required to compute the flow in porous media. Overall, a resolution of 200 × 200 pixels in the unit cell is necessitated to obtain reliable finite element solutions. It is worth noticing that simulations are performed using an Intel Xeon(R) E3-1505M 2.80GHz - 8 processors and 64GB RAM. Each simulation requires, in general, 30 minutes of computation time and about 6GB RAM, mostly dedicated to deal with the linear system (Eq. 6).

Table 1. Comparison of the solutions calculated by the finite element method and analytical solutions

Case of transversal flow through the unit cell				
Dim.	K_f	K_f (Analytic)	K_D	K_D (Analytic)
50	9.2317E-07	1.0000E-06	1.0000E-06	1.0000E-06
100	9.8415E-07	1.0000E-06	1.0000E-06	1.0000E-06
150	1.0271E-06	1.0000E-06	1.0000E-06	1.0000E-06
200	1.0001E-06	1.0000E-06	1.0000E-06	1.0000E-06
250	1.0000E-06	1.0000E-06	1.0000E-06	1.0000E-06
300	1.0000E-06	1.0000E-06	1.0000E-06	1.0000E-06
Case of longitudinal flow through the unit cell				
Dim.	K_f	K_f (Analytic)	K_D	K_D (Analytic)
50	9.2160E-03	1.0417E-02	5.2000E-07	5.0000E-07
100	1.0839E-02	1.0417E-02	4.9333E-07	5.0000E-07
150	1.0169E-02	1.0417E-02	5.0400E-07	5.0000E-07
200	1.0417E-02	1.0417E-02	5.0000E-07	5.0000E-07
250	1.0417E-02	1.0417E-02	5.0000E-07	5.0000E-07
300	1.0417E-02	1.0417E-02	5.0000E-07	5.0000E-07

Considering the longitudinal flow, Fig. 4 presents a comparison of the solutions obtained with the finite element method and analytical solutions derived from the previous section. The local velocity fields of the fluid and porous media are in excellent coherent with those obtained by the analytical solutions. A Poiseuille velocity profile is obtained, and the maximum velocity at y = 0 is reached (i.e., the value of 0.03125). Such a result is also the value obtained by the benchmark problem (see Eq. (11)). Fig. 5 shows the velocity profile concerning the longitudinal flow in the whole unit cell. It is worth noticing that the resolution is taken as 300 × 300 pixels. It can be seen that the Poiseuille profile is conserved in the fluid region, whereas constant values of the velocity field in the porous media are confirmed. In this case, the flow in the direction O_2 is null.

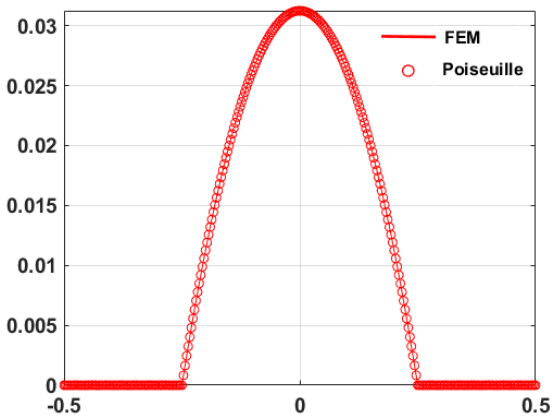

Figure 4. Comparison of finite element solutions and analytical solutions

Concerning the case of transversal flow, Fig. 6 presents a comparison of the solutions obtained by the finite element method and analytical solutions. The local velocity fields of the fluid and porous media are similar and in agreement with those obtained by the analytical solutions. A small difference in the border of the fluid region is observed. However, the errors between the solutions by the finite element method and analytical ones are small. The velocity profile concerning the longitudinal flow exhibits almost identical values in the whole unit cell of 300 × 300 pixels. Again, the flow in the direction O_2 is null. Overall, the choice of the element is reliable, and the solutions obtained by the finite element method are in excellent agreement with the developed analytical results.

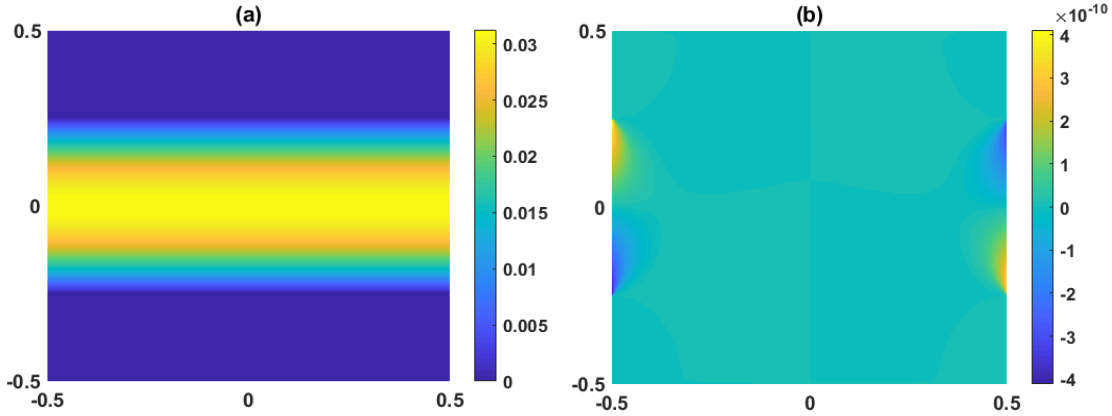

Figure 5. Local velocity profile of the longitudinal flow through the unit cell: (a) velocity field following direction O_1; and (b) velocity field following direction O_2

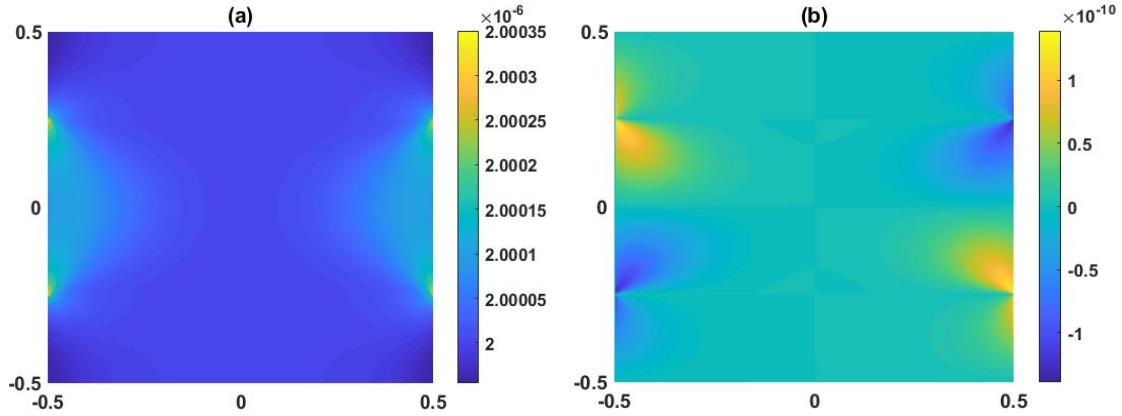

Figure 6. Local velocity profile of the transversal flow through the unit cell: (a) velocity field following direction O_1; and (b) velocity field following direction O_2

6. Discussions

Several discussions are given in this section.

First, considering the finite element method, an appropriate discretization is a crucial factor to obtain reliable results. In this study, the effect of the macroscopic permeability on the discretization choice is conducted. An excellent agreement between the numerical and analytical responses are achieved when the discretization of the unit cell is higher than 200 × 200 pixels. It is worth noticing that for 2-dimensional problems, a discretization of 200 × 200 pixels might pose no problem in terms of computational memory demand. However, considering 3-dimensional problems, a discretization of 200 × 200 × 200 voxels would require many efforts in terms of computational memory usage, especially when reversing the assembly matrix of the linear system. An extension of the present study is to treat the flow in a 3D unit cell, thus, an alternative solver for such a linear system should be investigated and implemented.

Second, it can be seen that for longitudinal flow, the flow in the Stokes region is a dominant one, whereas the flow in the Darcy region is almost null. In this case, the flow in the Stokes region plays a significant role in the macroscopic permeability of the fractured porous media. The permeability of the Darcy region only acts as a small correction to the macroscopic permeability. This situation can be seen in the field of geoscience, where the flow and transport of substances usually take place preferentially through an interconnected network of fractures (Hunt and Sahimi, 2017). Investigation on the macroscopic response of the flow in such porous media is crucial for understanding and modeling subsurface transport (Miglio et al., 2003). The finite element numerical tool developed in this study could be used for further study, especially the effect of the size of fractures on the macroscopic permeability. This is helpful in many engineering applications or geoscience as fractures are present in almost porous media like soil, rocks, glaciers, or porous materials such as wood.

Third, considering the transversal flow, it seems that for the considered case, the contribution of the two regions to the macroscopic permeability is similar. Besides, the velocity field shows that the flow is identical in the whole unit cell with only an inconsiderable difference at the border of the Stokes-Darcy region. The transversal flow, in this case, reflects a porous medium containing non-interconnected fractures (the so-called isolated or closed voids), in which the morphology of fractures plays a vital role in the substance transfer process in porous media. The morphology is thus a key parameter that determines the contribution of each region to the macroscopic permeability (Discacciati et al., 2002). Again, it is thus interesting to study the effect of the fracture morphology on the overall transport properties of porous media. Accurately capture the effect of a complex fracture network could enhance the knowledge of the fluid transfer process, which might be helpful in controlling groundwater flows or flow in naturally fractured reservoirs (Royer et al., 1996).

7. Conclusions

In this study, the development of a numerical tool based on the finite element method to solve the problem of fluid flow in fractured porous media is conducted. Fluid flow in porous media is considered as the coupling problem of the Stokes and Darcy equations, where the strong formulation is given. The variational formulation is then deduced, focusing on the Beavers-Joseph-Saffman boundary conditions at the interface between the two regions. A numerical

implementation of the variational formulation is next proposed, using the "robust" square elements to discretize the unit cell problem with periodic boundary conditions. The analytical solutions are also constructed in order to compare with the responses given by the numerical tool. The results show that the "robust element" could well simulate the flow behavior, both at the local field (i.e., the velocity and pressure field) and macroscopic properties.

Two perspectives of the present finite element toolbox, or this work, can be envisioned: (i) investigate the effect of fractures, including shape and size, on the flow and macroscopic behavior of porous media, and (ii) consider more realistic fractured porous media.

Acknowledgments

This research is funded by Vietnam National Foundation for Science and Technology Development (NAFOSTED) under grant number 107.03-2019.23

References

Arbogast T., Brunson D.S., 2007. A computational method for approximating a Darcy-Stokes system governing a vuggy porous medium. Computational Geosciences, 11, 207-218.

Auriaul J.-L., Sanchez-Palencia E., 1977. Etude du comportement macroscopique d'un milieu poreux saturé déformable. Journal de mécanique, 16, 575-603.

Auriault J.L., Boutin C., 1993. Deformable porous media with double porosity. Quasi-statics. II: Memory effects. Transport in porous media, 10, 153-169.

Auriault J.L., Boutin C., 1994. Deformable porous media with double porosity III: Acoustics. Transport in Porous Media, 14, 143-162.

Auriault J.L., Boutin, C., 1992. Deformable porous media with double porosity. Quasi-statics. I: Coupling effects. Transport in porous media, 7, 63-82.

Bachu S., 2008. CO_2 storage in geological media: Role, means, status and barriers to deployment. Progress in Energy and Combustion Science, 34, 254-273. https://doi.org/10.1016/j.pecs.2007.10.001

Beavers G.S., Joseph D.D., 1967. Boundary conditions at a naturally permeable wall. Journal of Fluid Mechanics, 30, 197-207.

Bose S., Roy M., Bandyopadhyay A., 2012. Recent advances in bone tissue engineering scaffolds. Trends in Biotechnology, 30, 546-554. https://doi.org/10.1016/j.tibtech.2012.07.005

Burman E., Hansbo P., 2007. A unified stabilized method for Stokes' and Darcy's equations. Journal of Computational and Applied Mathematics, 198, 35-51.

Celle P., Drapier S., Bergheau J.-M., 2008. Numerical modelling of liquid infusion into fibrous media undergoing compaction. European Journal of Mechanics-A/Solids, 27, 647-661.

Correa M.R., Loula A.F.D., 2009. A unified mixed formulation naturally coupling Stokes and Darcy flows. Computer Methods in Applied Mechanics and Engineering, 198, 2710-2722.

de Borst R., 2017. Fluid flow in fractured and fracturing porous media: A unified view. Mechanics Research Communications, Multi-Physics of Solids at Fracture, 80, 47-57. https://doi.org/10.1016/j.mechrescom.2016.05.004.

Dietrich P., Helmig R., Sauter M., Hötzl H., Köngeter J., Teutsch G., 2005. Flow and transport in fractured porous media. Springer Science & Business Media.

Discacciati M., Miglio E., Quarteroni A., 2002. Mathematical and numerical models for coupling surface and groundwater flows. Applied Numerical Mathematics, 43, 57-74.

Discacciati M., Quarteron A., Vall A., 2007. Robin-Robin domain decomposition methods for the Stokes-Darcy coupling. SIAM Journal on Numerical Analysis, 45, 1246-1268.

Herzi J.P., Lecler D.M., Gof P. Le., 1970. Flow of Suspensions through Porous Media-Application to Deep Filtration. Industrial & Engineering Chemistry, 62, 8-35. https://doi.org/10.1021/ie50725a003.

Hunt A.G., Sahim M., 2017. Flow, transport, and reaction in porous media: Percolation scaling, critical-path analysis, and effective medium approximation. Reviews of Geophysics, 55, 993-1078.

Karper T., Mardal K.-A., Winther R., 2009. Unified finite element discretizations of coupled Darcy-Stokes flow. Numerical Methods for Partial Differential Equations: An International Journal, 25, 311-326.

Layton W.J., Schieweck F., Yotov I., 2002. Coupling fluid flow with porous media flow. SIAM Journal on Numerical Analysis, 40, 2195-2218.

Ly H.-B., Le Droumaguet B., Monchiet V., Grande D. 2015. Designing and modeling doubly porous polymeric materials. The European Physical Journal Special Topics, 224, 1689-1706.

Ly H.B., Le Droumaguet B., Monchiet V., Grande D., 2015. Facile fabrication of doubly porous polymeric materials with controlled nano-and macro-porosity. Polymer, 78, 13-21.

Ly H.B., Le Droumaguet B., Monchiet V., Grande D., 2016a. Tailoring doubly porous poly (2-hydroxyethyl methacrylate)-based materials via thermally induced phase separation. Polymer, 86, 138-146.

Ly H.B., Monchiet V., Grande D., Lewis R.W., 2016b. Computation of permeability with Fast Fourier Transform from 3-D digital images of porous microstructures. International Journal of Numerical Methods for Heat & Fluid Flow, 26.

Miglio E., Quarteroni A., Saleri F., 2003. Coupling of free surface and groundwater flows. Computers & Fluids, 32, 73-83.

Mikelic A., Jäger W., 2000. On the interface boundary condition of Beavers, Joseph, and Saffman. SIAM Journal on Applied Mathematics, 60, 1111-1127.

Monchiet V., Bonnet G., Lauriat G., 2009. A FFT-based method to compute the permeability induced by a Stokes slip flow through a porous medium. Comptes Rendus Mécanique, 337, 192-197.

Monchiet V., Ly H.-B., Grande D., 2019. Macroscopic permeability of doubly porous materials with cylindrical and spherical macropores. Meccanica, 54, 1583-1596.

Nguyen T.-K., Monchiet V., Bonnet G., 2013. A Fourier based numerical method for computing the dynamic permeability of periodic porous media. European Journal of Mechanics-B/Fluids, 37, 90-98.

Pan C., Hilpert M., Miller C.T., 2004. Lattice-Boltzmann simulation of two-phase flow in porous media. Water Resources Research, 40.

Rahm D., 2011. Regulating hydraulic fracturing in shale gas plays: The case of Texas. Energy Policy, 39, 2974-2981. https://doi.org/10.1016/j.enpol.2011.03.009.

Royer P., Auriault J.-L., Boutin C., 1996. Macroscopic modeling of double-porosity reservoirs. Journal of Petroleum Science and Engineering, 16, 187-202.

Wang C.Y., 2001. Stokes flow through a rectangular array of circular cylinders. Fluid Dynamics Research, 29, 65-80.

https://doi.org/10.1016/S0169-5983(01)00013-2.

Wang C.Y., 2003. Stokes slip flow through square and triangular arrays of circular cylinders. Fluid Dynamics Research, 32, 233-246. https://doi.org/10.1016/S0169-5983(03)00049-2.

Whitaker S., 1967. Diffusion and dispersion in porous media. AIChE Journal, 13, 420-427. https://doi.org/10.1002/aic.690130308.

Xie X., Xu J., Xue G., 2008. Uniformly-stable finite element methods for Darcy-Stokes-Brinkman models. Journal of Computational Math ematics, 437-455.